Multi-Frequency Rational Sparse Array for Direction-of-Arrival Estimation

Yimin D. Zhang [1] and Moeness G. Amin [2]

[1] Department of Electrical and Computer Engineering, Temple University, Philadelphia, PA 19122, USA
[2] Department of Electrical and Computer Engineering, Villanova University, Villanova, PA 19085, USA

***Abstract*—In this paper, we consider sparse array-based direction-of-arrival (DOA) estimation using multiple frequencies that are associated with coprime rational numbers. By exploiting rational frequencies instead of integer ones as used in the existing literature, the proposed method provides a flexible design of multi-frequency sparse arrays with a reduced frequency separation. We demonstrate that the use of coprime rational frequencies ensures unambiguous DOA estimation, despite that the interelement spacing of the array in each frequency is higher than half-wavelength. We further consider practical selection of the rational frequencies guided by the spatial correlation coefficient.**

Keywords: Direction-of-arrival estimation, sparse array, rational analysis, multi-frequency array design, spatial correlation coefficient.

I. Introduction

Direction-of-arrival (DOA) estimation is an important application of array signal processing which determines the spatial spectrum of impinging electromagnetic waves [1, 2]. An N-element uniform linear array (ULA) offers $N-1$ degrees-of-freedom (DOFs) and conventional DOA estimation methods, such as MUSIC and ESPRIT, can be used to resolve up to $N-1$ sources or targets. Conversely, sparse placement of array sensors can achieve a higher number of DOFs, allowing the resolution of more targets with the same number of sensors [3, 4]. Typically, an increased number of DOFs is accomplished by leveraging the extended difference coarray, which uses lag differences between physical sensors to determine the virtual sensor positions. The development of the nested array [5] and the coprime array [6] has ignited the wave of studying systematical sparse array design and processing in the past decade.

By utilizing frequency diversity, multi-frequency array designs provide a useful approach for implementing sparse arrays in a more effective manner. Because the array manifold is associated with the signal carrier frequency, a virtual coprime array is created using a single ULA with two frequencies [7]. When these two frequencies have a coprime relationship, the signals observed at the ULA using the two frequencies are similar to those observed at a coprime array consisting of two physical uniform linear subarrays. As such, applying frequency diversity to sparse arrays allows for greater flexibility in array design with significantly reduced complexity. The extension to multiple coprime frequencies, along with an analysis of the achievable number of DOFs, is provided in [8–10]. In [11], a technique is developed to rapidly estimate DOAs using a multi-frequency sparse ULA when the number of sources is less than that of physical sensors. Additionally, the Cramer-Rao lower bound of the dual-frequency coprime array is analyzed in [12, 13].

In [14–16], a general framework of multi-frequency sparse array design is developed for signal DOA estimation with a significantly higher number of DOFs. This is achieved by designing the multi-frequency sparse arrays to have zero lag redundancy in the rendered difference coarray. A modified sensor interpolation technique is developed to accurately estimate the signal correlation matrix so that the effect of holes in the difference coarray is mitigated [16].

While the array designs provided in [14–16] are effective in terms of the achieved number of DOFs, array design based on the zero-lag redundancy requirement makes it highly restrictive. For example, such designs may require a high frequency separation which is not always feasible in practice. The recent development of the rational array design [17, 18] provides a new direction of sparse array design. In this paper, we apply the concept of rational sparse arrays to multi-frequency-based sparse array design, resulting in generalized multi-frequency rational sparse arrays. Such generalization provides a flexible design of multi-frequency sparse arrays with a reduced frequency separation. We demonstrate that the use of rational frequencies ensures unambiguous DOA estimation, despite that the inter-element spacing in each frequency is higher than half-wavelength. Guided by the spatial correlation coefficient, we further consider practical selection of the rational frequencies.

Notations: We use lower-case (upper-case) bold characters to denote vectors (matrices). In particular, $\boldsymbol{I}_N$ denotes the $N \times N$ identity matrix. $(.)^{\mathrm{T}}$ and $(.)^{\mathrm{H}}$ respectively represent the transpose and conjugate transpose of a matrix or a vector. (a, b) or $\gcd(a, b)$ denotes the greatest common divisor (GCD) of two integers a and b, so $(a, b) = 1$ means that the integers are coprime. $\mathrm{lcm}(a, b)$ denotes the least common multiple (LCM) of integers a and b.

II. Multi-Frequency Rational Sparse Arrays

We consider a DOA estimation problem by simultaneously emitting I continuous wave signals with frequencies of $f_i, i = 1, 2, \cdots, I$, from a single transmit antenna or a phased array. Extension to multiple transmitter cases is straightforward based on the multiple-input multiple-output (MIMO) radar concept [19]. Assume an N-sensor ULA with interelement spacing d, i.e., the locations of the N physical sensors are

$$\boldsymbol{z}_0 = [0, d, 2d, \cdots, (N-1)d]^{\mathrm{T}}. \tag{1}$$

When the carrier frequency is f_i and the corresponding wavelength is $\lambda_i = c/f_i$ with c denoting the propagation speed of the electromagnetic wave, we express d as the multiple of half-wavelength as $d = M_i\lambda_i/2$. In [14–16], we assumed that M_i are integers so that all physical sensors are located on the half-wavelength grid. In this paper, we generalize the concept to rational arrays [17, 18] so that M_i are rational values such that $M_i = P_i/Q_i$ with P_i and Q_i being integers. As such, the scenarios considered in [14–16] become a special case of the rational array by setting Q_i to take integer values for all $i = 1, \cdots, I$.

For K far-field targets whose respective DOAs are $\theta_1, \cdots, \theta_K$, the return signal vector associated with the ith frequency component is expressed as:

$$\tilde{\boldsymbol{x}}_i(t) = e^{j2\pi f_i t}\sum_{k=1}^{K}\rho_k^{(i)}(t)\boldsymbol{a}_i(\theta_k) + \tilde{\boldsymbol{n}}_i(t), \tag{2}$$

where $\rho_k^{(i)}(t)$ is the reflection coefficient which is in general frequency-dependent because both phase delay and target reflectivity vary with frequency. In addition,

$$\boldsymbol{a}_i(\theta_k) = \left[1,\ e^{\ j\frac{2\pi d}{\lambda_i}\sin(\theta_k)}, \cdots, e^{\ j\frac{2\pi(N-1)d}{\lambda_i}\sin(\theta_k)}\right]^{\mathrm{T}} \tag{3}$$

is the steering vector corresponding to θ_k. In addition, $\tilde{\boldsymbol{n}}_i(t) \sim \mathcal{CN}(0, \sigma_n^{(i)}\boldsymbol{I}_N)$ denotes the additive white Gaussian noise.

After demodulating the signal vector using carrier frequency f_i, we obtain the baseband signal vector as

$$\boldsymbol{x}_i(t) = \sum_{k=1}^{K}\rho_k^{i}(t)\boldsymbol{a}_i(\theta_k) + \boldsymbol{n}_i(t) = \boldsymbol{A}_i\boldsymbol{s}_i(t) + \boldsymbol{n}_i(t), \tag{4}$$

where $\boldsymbol{A}_i = [\boldsymbol{a}_i(\theta_1), ..., \boldsymbol{a}_i(\theta_K)]$ and $\boldsymbol{s}_i(t) = [\rho_1^{(i)}, ..., \rho_K^{(i)}]^{\mathrm{T}}$. To simplify the notation, we denote $\omega_k = \pi\sin(\theta_k)$. Using $M_i = 2d/\lambda_i$, we have

$$\boldsymbol{a}_i(\theta_k) = \left[1,\ e^{\ jM_i\omega_k}, \cdots, e^{\ j(N-1)M_i\omega_k}\right]^{\mathrm{T}}. \tag{5}$$

For the ith frequency, the sensors positions, normalized with half-wavelength in each frequency, is expressed as

$$\tilde{\boldsymbol{z}}_i = \frac{2\boldsymbol{z}_0}{\lambda_i} = [0, M_i, \cdots, (N-1)M_i]^{\mathrm{T}}, \tag{6}$$

and the combined virtual sensor locations contributed by all the I frequencies becomes

$$\tilde{\boldsymbol{z}} = [\tilde{\boldsymbol{z}}_1^{\mathrm{T}}, \tilde{\boldsymbol{z}}_2^{\mathrm{T}}, \cdots, \tilde{\boldsymbol{z}}_I^{\mathrm{T}}]^{\mathrm{T}}. \tag{7}$$

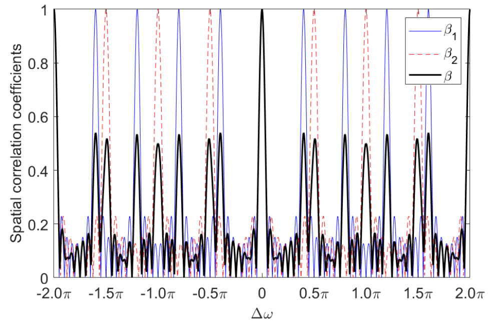

Fig. 1: Spatial correlation coefficients for an 8-element ULA.

III. Identifiability Analysis

A. Spatial Correlation Coefficient

For simplicity and without loss generality, we consider the case of $I = 2$ frequencies. Furthermore, we only consider the case that $\rho_k^{(i)}(t)$ does not vary with frequency. This is referred to as the proportional spectra scenario in [20]. In this case, $\boldsymbol{s}_1(t) = \boldsymbol{s}_2(t) \triangleq \boldsymbol{s}(t)$, and stacking $\boldsymbol{x}_1(t)$ and $\boldsymbol{x}_2(t)$ renders

$$\begin{aligned}\boldsymbol{x}(t) &= \begin{bmatrix}\boldsymbol{x}_1(t)\\ \boldsymbol{x}_2(t)\end{bmatrix} = \begin{bmatrix}\boldsymbol{A}_1\boldsymbol{s}_1(t)\\ \boldsymbol{A}_2\boldsymbol{s}_2(t)\end{bmatrix} + \boldsymbol{n}(t)\\ &= \begin{bmatrix}\boldsymbol{A}_1\\ \boldsymbol{A}_2\end{bmatrix}\boldsymbol{s}(t) + \boldsymbol{n}(t) = \boldsymbol{A}\boldsymbol{s}(t) + \boldsymbol{n}(t),\end{aligned} \tag{8}$$

where $\boldsymbol{A} = [\boldsymbol{A}_1^{\mathrm{T}}\ \ \boldsymbol{A}_2^{\mathrm{T}}]^{\mathrm{T}}$, and the corresponding steering vector is

$$\boldsymbol{a}(\theta_k) = [\boldsymbol{a}_1^{\mathrm{T}}(\theta_k)\ \ \boldsymbol{a}_2^{\mathrm{T}}(\theta_k)]^{\mathrm{T}}. \tag{9}$$

To perform DOA estimation unambiguously, we need to have $\boldsymbol{a}(\theta_k) \neq \boldsymbol{a}(\theta_l)$ for any $\theta_k \neq \theta_l$. Because $\boldsymbol{a}(\theta_k)$ consists of two parts, namely, $\boldsymbol{a}_1(\theta_k)$ and $\boldsymbol{a}_2(\theta_k)$, respectively corresponding to the two frequencies, the unambiguous DOA estimation condition is equivalent to $\boldsymbol{a}_1(\theta_k) \neq \boldsymbol{a}_1(\theta_l)$ *or* $\boldsymbol{a}_2(\theta_k) \neq \boldsymbol{a}_2(\theta_l)$.

Further, the unambiguous DOA estimation condition $\boldsymbol{a}(\theta_k) \neq \boldsymbol{a}(\theta_l)$ can be equivalently considered that the spatial correlation coefficient between θ_k and θ_l, defined as [21]

$$\begin{aligned}\beta_{k,l} &= \frac{1}{2N}\left|\boldsymbol{a}^{\mathrm{H}}(\theta_k)\boldsymbol{a}(\theta_l)\right|\\ &= \frac{1}{2N}\left|\boldsymbol{a}_1^{\mathrm{H}}(\theta_k)\boldsymbol{a}_1(\theta_l) + \boldsymbol{a}_2^{\mathrm{H}}(\theta_k)\boldsymbol{a}_2(\theta_l)\right|,\end{aligned} \tag{10}$$

is less than unity for all $k \neq l$. In other words, a necessary condition for ambiguity to occur is when the spatial correlation coefficient of both subarrays is unity, i.e., $|\boldsymbol{a}_i^{\mathrm{H}}(\theta_k)\boldsymbol{a}_i(\theta_l)|/N = 1$ for some $k \neq l$ for both $i = 1, 2$.

This important property was emphasized in the design of coprime array [6]. As an example, we show in Fig. 1 for an 8-element ULA that, while the subarrays with $M_1 = 5$ and $M_2 = 4$ show grating peaks with unit spatial correlation coefficients ($\beta_{k,l}^{(1)} = 1$ or $\beta_{k,l}^{(2)} = 1$), the spatial correlation coefficient β of the array consisting of both frequencies does not have an ambiguity issue.

B. Identifiability Analysis

Denote $\Delta\omega = \omega_l - \omega_k$ with $l \neq k$. The spatial correlation coefficient of a subarray corresponding to frequency f_i, i.e.,

$$\frac{1}{N}\boldsymbol{a}_i^{\mathrm{H}}(\theta_k)\boldsymbol{a}_i(\theta_l) = \frac{1}{N}\sum_{n=0}^{N-1} e^{jM_i\Delta\omega n}, \tag{11}$$

becomes unity only when $M_i\Delta\omega = 2\pi U$, where $U \neq 0$ is an integer. As θ varies within the range of $\theta \in [-\pi/2, \pi/2)$, $\omega \in [-\pi, \pi)$ and $\Delta\omega \in (-2\pi, 2\pi)$. In a conventional ULA satisfying the Nyquist sampling condition, i.e., $M_i \leq 1$, the above ambiguity condition cannot be satisfied, thus guaranteeing unambiguous DOA estimation.

When $M_i = P_i/Q_i > 1$, the ambiguity condition for the subarray corresponding to the ith frequency becomes $\Delta\omega = 2\pi U/M_i = 2\pi U Q_i/P_i$. In this case, ambiguity occurs if only one frequency is used. However, in the case of two frequencies, unambiguous DOA estimation can still be achieved.

The spatial correlation coefficient can be expressed as

$$\beta_{k,l} = \frac{1}{2N}\left|\sum_{n=0}^{N-1}\left(e^{jM_1\Delta\omega n} + e^{jM_2\Delta\omega n}\right)\right|. \tag{12}$$

When $U_1Q_1/P_1 \neq U_2Q_2/P_2$ for any integers U_1 and U_2, DOA estimation is unambiguous because this violates the ambiguous DOA estimation condition even if one of the two subarrays has a unit subarray spatial correlation coefficient.

Define the GCD of two positive rational numbers $M_1 = P_1/Q_1$ and $M_2 = P_2/Q_2$ as [17, 18]

$$\gcd(M_1, M_2) = \frac{\gcd(P_1, P_2)}{\mathrm{lcm}(Q_1, Q_2)}. \tag{13}$$

Positive rational numbers M_1 and M_2 are said to be coprime when $\gcd(M_1, M_2) < 1$. With these definitions, unambiguous DOA estimation is achieved when M_1 and M_2 are coprime.

IV. Simulation Results

A. Spatial Correlation Coefficient

Because P_1, Q_1, P_2, and Q_2 can be flexibly chosen, the required stated above leaves a large region for the selection of rational values M_1 and M_2 that guarantee unambiguous DOA estimation. However, it is important to properly choose M_1 and M_2 so that the maximum value of the spatial correlation coefficient $\beta_{k,l}$, which is abbreviated as β in the sequel, is kept low throughout the sidelobe regions.

In Fig. 2(a), we show the spatial correlation coefficient of the array where we fix $M_1 = 2$, i.e., $P_1 = 2$ and $Q_1 = 1$, and vary M_2 between 0 and 8. Several important facts can be observed here. First, the mainlobe is located at $\Delta\omega = 0$ and the width narrows as M_2 increases, i.e., the overall array aperture increases. Second, because of the specific value of $M_1 = 2$, the first subarray corresponding to frequency f_1 contributes a value of 0.5 towards β when $\Delta\omega$ takes values around -2π, $-\pi$, π and 2π. When the second subarray corresponding to frequency f_2 contributes a value of 0.5 towards the same

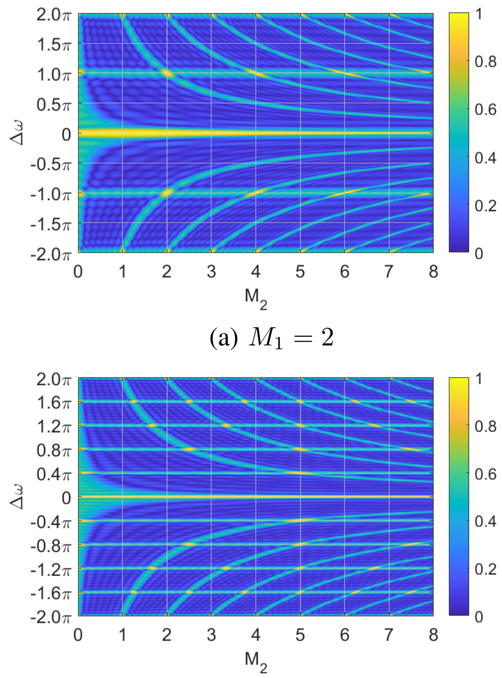

(a) $M_1 = 2$

(b) $M_1 = 5$

Fig. 2: Spatial correlation coefficients versus M_2 for an 8-element ULA.

region, as observed at $M_2 = 2, 4, 6$, and 8, β becomes 1 and ambiguity occurs. It is interesting to notice that, as the value of M_2 increases, the intersected region becomes broader.

Fig. 2(b) shows similar results for the case of $M_1 = 5$. In this case, the first subarray corresponding to frequency f_1 contributes a value of 0.5 towards β when $\Delta\omega$ is a multiple of 0.4π and β takes a value of unity at more (M_1, M_2) pairs. The intersection region becomes broader for small values of $\Delta\omega$ values as demonstrated for $\Delta\omega = \pm 0.4\pi$ and $M_2 = 5$.

From Fig. 2(b), we can observe that M_2 can take a fractional value around $M_1 = 5$ to achieve a low spatial correlation coefficient. Fig. 3 shows the results for $M_2 = 4.6$. The highest sidelobe level in this case is below 0.6, which is considered insignificant in DOA estimation [21]. In this way, the separation between the two frequencies is only 8.33%, which is much smaller than 22.2% if M_2 is constrained to integers and takes the next smaller integer value of $M_2 = 4$ (Note that we assume $M_2 > M_1$ to keep the same array aperture as M_2 varies). Such flexibility in choosing a smaller frequency separation makes it much easier to apply the multi-frequency sparse array concept in applications where the available bandwidth is limited.

B. Difference Coarray Lags

We now compare the difference coarray lags obtained from the rational array configuration with $M_1 = 5$ and $M_2 = 4.6 = 23/5$, and compare them with those obtained from an array using an integer value of $M_1 = 5$ and $M_2 = 4$. As we kept $\max(M_1, M_2)$ identical for both array configurations in

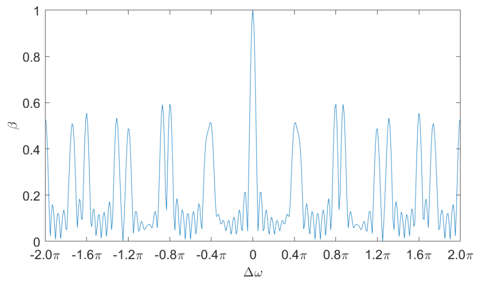

Fig. 3: Spatial correlation coefficient when $M_1 = 5$ and $M_2 = 4.6$ for an 8-element ULA.

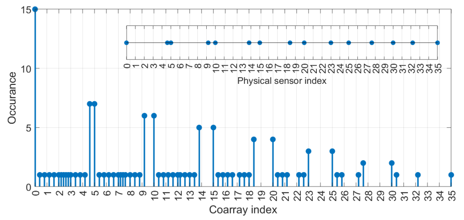

(a) $M_1 = 5, M_2 = 4.6$

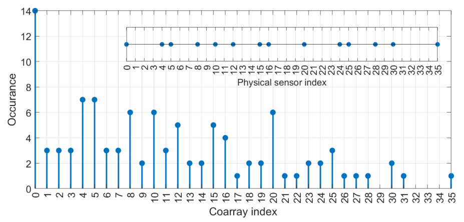

(b) $M_1 = 5, M_2 = 4$

Fig. 4: Difference coarray lags for an 8-element array.

this case, the aperture is the same. It is seen in Fig. 4 that the rational array achieves more densely distributed lags with smaller gaps. While the exact analysis of the DOFs for such lags off the half-wavelength is not straightforward and will be considered in our future work, in this specific case, the rational array achieves a comparable set of lag occupancy in the grid of half-wavelength spacing.

V. Conclusion

In this paper, we have proposed the use of multiple rational frequencies for sparse array-based DOA estimation. By generalizing the conventional multi-frequency sparse arrays, which only use frequencies with an integer relationship, to those with rational numbers, an apparent advantage of the proposed approach is the flexible frequency selection, thereby enabling its use when a wide separation is infeasible. We have examined the unambiguous DOA estimation conditions, the spatial correlation coefficient, and the difference coarray lags.

VI. References

[1] H. L. Van Trees, *Optimum Array Processing: Part IV of Detection, Estimation, and Modulation Theory*. Wiley, 2002.

[2] E. Tuncer and B. Friedlander (eds), *Classical and Modern Direction of Arrival Estimation*. Academic Press, 2009.

[3] A. Moffet, “Minimum-redundancy linear arrays,” *IEEE Trans. Antennas Propagat.*, vol. 16, no. 2, pp. 172-–175, March 1968.

[4] R. T. Hoctor and S. A. Kassam, “The unifying role of the co-array in aperture synthesis for coherent and incoherent imaging,” *Proc. IEEE*, vol. 78, no. 4, pp. 735-–752, April 1990.

[5] P. Pal and P. P. Vaidyanathan, “Nested arrays: A novel approach to array processing with enhanced degrees of freedom,” *IEEE Trans. Signal Process.*, vol. 58, no. 8, pp. 4167–4181, Aug. 2010.

[6] P. P. Vaidyanathan and P. Pal, “Sparse sensing with co-prime samplers and arrays,” *IEEE Trans. Signal Process.*, vol. 59, no. 2, pp. 573-586, Feb. 2011.

[7] Y. D. Zhang, M. G. Amin, F. Ahmad, and B. Himed, “DOA estimation using a sparse uniform linear array with two CW signals of co-prime frequencies,” in *Proc. IEEE Int. Workshop CAMSAP*, Saint Martin, Dec. 2013, pp. 404–407.

[8] S. Qin, Y. D. Zhang, and M. G. Amin, “DOA estimation exploiting coprime frequencies,” in *Proc. SPIE*, vol. 9103, no. 91030E, Baltimore, MD, May 2014.

[9] S. Qin, Y. D. Zhang, M. G. Amin, and B. Himed, “DOA estimation exploiting a uniform linear array with multiple co-prime frequencies,” *Signal Process.*, vol. 130, pp. 37–46, Jan. 2017.

[10] A. Ahmed, Y. D. Zhang, and B. Himed, “Cumulant-based direction-of-arrival estimation using multiple co-prime frequencies,” in *Proc. Asilomar Conf. Signals, Syst., Comput.,* Pacific Grove, CA, Oct. 2017, pp. 1188–1192.

[11] A. Liu, X. Zhang, Q. Yang, and W. Deng, “Fast DOA estimation algorithms for sparse uniform linear array with multiple integer frequencies,” *IEEE Access*, vol. 6, pp. 29952–29965, May 2018.

[12] M. Guo, Y. D. Zhang, and T. Chen, “Performance analysis for uniform linear arrays exploiting two coprime frequencies,” *IEEE Signal Process. Lett.*, vol. 25, no. 6, pp. 838–842, June 2018.

[13] Y. Liang, W. Cui, Q. Shen, W. Liu, and H. Wu, “Cramér-Rao bound for DOA estimation exploiting multiple frequency pairs,” *IEEE Signal Process. Lett.*, vol. 28, pp. 1210–1214, 2021.

[14] S. Zhang, A. Ahmed, Y. D. Zhang, and S. Sun, “DOA estimation exploiting interpolated multi-frequency sparse array,” in *Proc. IEEE Sensor Array and Multich. Signal Process. Workshop*, Hangzhou, China, June 2020.

[15] A. Ahmed, D. Silage, and Y. D. Zhang, “High-resolution target sensing using multi-frequency sparse array,” in *Proc. IEEE Sensor Array and Multich. Signal Process. Workshop*, Hangzhou, China, June 2020.

[16] S. Zhang, A. Ahmed, Y. D. Zhang, and S. Sun, “Enhanced DOA estimation exploiting multi-frequency sparse array,” *IEEE Trans. Signal Process.*, vol. 69, pp. 5935–5946, Oct. 2021.

[17] P. Kulkarni and P. P. Vaidyanathan, “Rational arrays for DOA estimation,” in *Proc. IEEE Int. Conf. Acoust. Speech Signal Process. (ICASSP)*, Singapore, Singapore, 2022, pp. 5008–5012.

[18] P. Kulkarni and P. P. Vaidyanathan, “Non-integer arrays for array signal processing,” *IEEE Trans. Signal Process.*, vol. 70, pp. 5457–5472, 2022.

[19] J. Li and P. Stoica, *MIMO Radar Signal Processing*. Wiley, 2008.

[20] E. BouDaher, Y. Jia, F. Ahmad, and M. G. Amin, “Multifrequency co-prime arrays for high-resolution direction-of-arrival estimation,” *IEEE Trans. Signal Process.*, vol. 63, no. 14, pp. 3797–3808, 2015.

[21] H-C. Lin, “Spatial correlations in adaptive arrays,” *IEEE Trans. Antennas Propagat.*, vol. 30, no. 2, pp. 212–223, March 1982.